# Correlation between surface and bulk orientations of liquid crystals on rubbed polymer surfaces: Odd-even effects of polymer spacer units

Diethelm Johannsmann,* Hitian Zhou,† Peter Sonderkaer,‡ Harald Wierenga,§ Bernt O. Myrvold,** and Y. R. Shen
*Department of Physics, University of California, Berkeley, California 94720*
(Received 22 February 1993)

Using surface optical second-harmonic generation, we have determined the molecular tilt angle and the in-plane orientational order of the liquid-crystal molecules 4′-*n*-octyl-4-cyanobiphenyl (8CB) on a series of polyimide surfaces. The polyimides differ in the length of the flexible spacers in between neighboring aromatic cores. Using birefringence measurements, we obtained the bulk tilt angle of liquid-crystal cells having the same series of surfaces. The surface molecular tilt angle, the in-plane orientational ordering near the surface, and the bulk tilt angle all exhibit an odd-even effect related to the odd or even number of spacer units in the polyimides. The results are explained by the fact that polyimide surfaces with even numbers of spacer units are smoother and capable of inducing higher surface ordering in the 8CB surface layer. The orientational order at the surface is shown to be intimately correlated with the bulk tilt angle.

PACS number(s): 61.30.Gd, 68.10.Cr, 07.60.−j, 42.65.An

## I. INTRODUCTION

Surface-induced orientation and alignment of liquid crystals (LC) is a subject of immense scientific and technological interest. It has been well established that the orientation of a LC bulk can be fully dictated by "surface anchoring" [1]. Phenomenological models have been proposed to explain the anchoring mechanism and the bulk alignment [2]. Proper surface treatment can presumably lead to a surface anchoring needed for a desired bulk alignment [3]. For example, conical surface anchoring with significant molecular tilt angle is believed to be ideal for the fabrication of supertwisted nematic cells [4].

Polyimide-coated substrates are often used in LC display devices. Rubbing the polyimide-coated surface induces the LC molecules to lie preferentially parallel to the rubbing direction [5–7], but the bulk alignment is usually at an angle from the surface plane [1]. This tilt angle may depend on the polyimide species coated on the surface. Yokokura *et al.* used polyimides composed of relatively flexible methylene spacers linking aromatic cores and found that the tilt angles are larger for even numbers of methylene spacer units and smaller for odd numbers [8]. They related this effect to the surface topology on a microscopic scale. Using x-ray scattering and scanning electron microscopy, they showed that the surface of a polyimide with an odd number of spacer units is microscopically more corrugated. They have proposed a molecular picture of the polyimide interface in which the first monolayer of LC molecules is expected to have a lower tilt angle if the surface is microscopically more corrugated. However, there is no experimental evidence available to support the model.

Recently, optical surface second-harmonic generation (SHG) has been developed as a versatile tool for studies of adsorbates at various interfaces [9]. In particular, it has the sensitivity to detect an adsorbed molecular monolayer and can be used to measure the average orientation of the monolayer [5]. It is therefore ideally suited for probing LC monolayers on polyimides. Indeed, using this technique, average orientations of 4′-*n*-octyl-4-cyanobiphenyl (8CB) monolayers on both rubbed and unrubbed polyimide-coated substrates have been measured [5]. Obviously, the same technique can be applied to the measurements of the orientations of LC monolayers on a series of polyimides and the results can be used to test the model of Yokokura *et al.* [8].

In this paper, we report on experimental investigations of the molecular orientations of 8CB monolayers on polyimide-coated substrates and of 8CB bulk material sandwiched between polyimide-coated substrates. The polyimides used are poly-*n*-alkylpyromellitic imides $-(N-(CO)_2-C_6H_2-(CO)_2-N-(CH_2)_n-)$ with $n=3$, 4, 5, and 6, similar to those used by Yokokura *et al.* [8]. The chemical structure of such polyimides is depicted in Fig. 1. We have observed an odd-even effect in the 8CB bulk molecular orientations similar to that reported by Yokokura *et al.*, although not as strong. We have also observed an odd-even effect in the molecular orientations of the surface monolayers, but it is

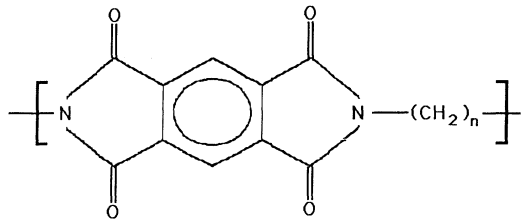


n = 3,4,5,6

FIG. 1. The chemical structure of the polyimides used in our experiment.

 

opposite to that found in the bulk. This is clearly at variance with the picture proposed by Yokokura *et al.* [8].

## II. SAMPLE PREPARATION AND EXPERIMENTAL ARRANGEMENT

We were interested in studying the effect of rubbed and unrubbed polymer surfaces on the monolayer and the bulk of 8CB. The polymers used were poly-*n*-propyl-pyromellitic imide (P3), poly-*n*-butyl-pyromellitic imide (P4), poly-*n*-pentyl-pyromellitic imide (P5), and poly-*n*-hexyl-pyromellitic imide (P6) (Fig. 1). The aromatic cores are connected by spacers of length between three and six methylene groups. Since the persistence length of polyethylene is in the same range as the spacer length, the spacers cannot be regarded as fully flexible and the orientations of neighboring pyromellitic units are correlated. An even number of spacer units favors parallel orientation of neighboring aromatic cores. The polymers are elongated locally, which tends to yield smoother surfaces as well as better crystallization [8,10]. In the case of an odd number of spacer units, the orientations of neighboring units generally differ. Surface corrugation could then occur on the molecular scale and crystallization is hindered [8].

The polyimide surfaces were prepared by spin coating the polyamic precursors onto fused silica plates with a spinning speed of 3000 rpm. The solvent was allowed to evaporate at 60 °C for 1 h. Subsequently the samples were baked at 200 °C for 2 h and cured at 300 °C for 5 h.

Monolayers of 8CB purchased from British Drug House (BDH) were prepared by spreading onto the polyimide-coated substrates out of solution in isopropyl-alcohol. Since the solvent wets the surface very well, a rather homogeneous monolayer can be obtained. The amount of 8CB used in the spread was chosen to yield a surface coverage slightly above one monolayer. As has been shown previously [11], the excess molecules would pair up to form quadrupoles and hence contribute very little to the second-harmonic signal. The 8CB cells were fabricated by sandwiching 8CB between two identically prepared polyimide-coated substrates. To ensure homogeneous bulk alignment, the two opposing polyimide surfaces were rubbed in opposite directions. Figure 2 schematically depicts the cells. The cell thickness was about 125 $\mu$m. The cells were filled with 8CB in the isotropic phase by capillary action. Samples with a single domain of 8CB in the smectic phase could be readily obtained. The quality of the samples was checked by visual inspection under a polarizing microscope.

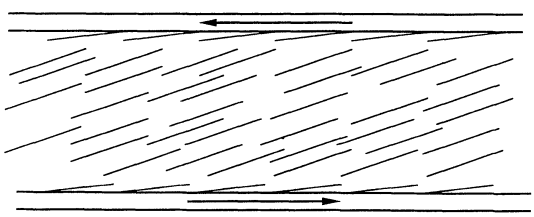

FIG. 2. Schematic picture of the homogeneously aligned liquid-crystal cells.

The experimental setup for the surface SHG measurements on molecular monolayers has been described elsewhere [9]. Briefly, a frequency-doubled $Q$-switched mode-locked Nd:YAG laser (where YAG denotes yttrium aluminum garnet) with a peak power of 500 kW, an energy of 600 $\mu$J/pulse, and a repetition frequency of 500 Hz was used as the source of the fundamental beam. The beam was focused to a spot of about 0.1 mm$^2$ on the sample, with an angle of incidence of 50°. A properly arranged polarizer-analyzer set specified the polarizations of the input and the output beam. The sample was mounted on a rotation stage, which was controlled by a stepping motor. This allowed the measurement of SHG as a function of sample rotation in the azimuthal plane. Four different sets of data were taken corresponding to four different combinations of input and output polarizations (s in–s out, p in–s out, s in–p out, and p in–p out). The SH output was detected by a photomultiplier after proper spectral filtering, followed by a gated integrator. The signal obtained was typically 1000 counts/min. The background was less than 10 counts/min.

Our measurement of the tilt angle $\theta_B$ of the bulk 8CB orientation relied on the effect that the LC director in the bulk of a mesophase does not change when a magnetic field is applied to the sample along the director [12]. In the setup, the sample was placed between two crossed polarizers to yield a conoscopic picture. The polarizer-sample-analyzer assembly on a rotatable mount was inserted between the poles of a strong electromagnet ($B_{\max}=1.5$ T). The temperature was 35.0±0.5 °C. No change in the conoscopic picture was observed, if the magnetic field was parallel to the LC director in the field-free state. This allowed us to measure the bulk LC orientation with a precision of about 0.5°.

## III. EXPERIMENTAL RESULTS AND DATA ANALYSIS

Consider first the tilt angle $\theta_B$ (from the surface plane) of the bulk 8CB orientation. We have used the technique described in Sec. II to measure $\theta_B$ of homogeneously aligned 8CB films sandwiched between substrates coated with different polyimides but similarly rubbed. The results obtained are $\theta_B=2.3°$, 4.3°, 2.7°, and 3.4° for substrates coated with polyimide P3, P4, P5, and P6, respectively. They show that surfaces coated with polyimides with even numbers of spacer units lead to higher bulk tilt angles, although the effect is not very strong. This is in agreement with what Yokokura *et al.* observed [8].

We have also measured the tilt angle $\theta_m$ (from the surface plane) of 8CB monolayers on both rubbed and unrubbed polyimide surfaces. This was achieved by measuring SHG from the monolayers with different input-output polarization combinations and analyzing the result as follows [5]. For 8CB on unrubbed surfaces, the molecular orientational distribution is azimuthally symmetric. The only nonvanishing nonlinear susceptibility elements are $\chi^{(2)}_{zzz}$, $\chi^{(2)}_{zxx}=\chi^{(2)}_{zyy}$, and $\chi^{(2)}_{xzx}=\chi^{(2)}_{yzy}$. It has been shown in previous work [5] that for 8CB monolayers, we have approximately $\vec{\vec{\chi}}^{(2)}=N\langle\vec{\vec{\alpha}}^{(2)}\rangle$ and the hyperpolarizability $\vec{\vec{\alpha}}^{(2)}$ is dominated by a single element $\alpha^{(2)}_{\zeta\zeta\zeta}$, where $N$ is the monolayer density, the angular

brackets denote an orientation average, and $\zeta$ is along the molecular axis. We find

$$\chi^{(2)}_{zzz}=N\alpha^{(2)}_{\zeta\zeta\zeta}\langle \sin^3\theta_m \rangle ,$$
$$\chi^{(2)}_{zyy}=\chi^{(2)}_{yzy}=\tfrac{1}{2}N\alpha^{(2)}_{\zeta\zeta\zeta}\langle \sin\theta_m \cos^2\theta_m \rangle . \quad (1)$$

One can deduce $\chi^{(2)}_{zzz}$ and $\chi^{(2)}_{zyy}$ from SHG measurements with (s in–p out) and (p in–p out) polarization combinations, following the equations given in Ref. [5]. For this purpose, we need to know the refractive indices of the quartz substrate and the polyimides as well as the thickness of the polyimide films. For fused quartz, the refractive indices at 532 and 266 nm are 1.46 and 1.5, respectively. Using ellipsometry and reflectivity measurements close to the Brewster angle, we obtained the refractive indices of the polyimides at 532 and 266 nm to be 1.7 and $2.2+i0.14$, respectively, and the film thickness to be about 270 nm. We also assume that the 8CB monolayer has a refractive index of 1.

The ratio of $\chi^{(2)}_{zyy}$ and $\chi^{(2)}_{zzz}$ is [5]

$$\frac{\chi^{(2)}_{zyy}}{\chi^{(2)}_{zzz}}=\frac{1}{2}\frac{\langle \sin\theta_m \cos^2\theta_m \rangle}{\langle \sin^3\theta_m \rangle}=\frac{1}{2}\left[\frac{\langle \sin\theta_m \rangle}{\langle \sin^3\theta_m \rangle}-1\right] . \quad (2)$$

If the orientational distribution is assumed to be a $\delta$ function, then the tilt angle $\theta_m$ can be deduced from the ratio. Thus from the measured values of $\chi^{(2)}_{zzz}$ and $\chi^{(2)}_{zyy}$ we find $\theta_m=18°$, 14°, 16°, and 12° for 8CB monolayers on P3, P4, P5, and P6 polyimide-coated surfaces. Again the existence of the odd-even effect in $\theta_m$ is obvious. However, the effect is opposite to that observed in $\theta_B$: $\theta_m$ is smaller, instead of larger, for polyimides with even numbers of spacer units. We also notice that $\theta_m$ tends to decrease with increasing number of spacer units.

For rubbed polyimide-coated surfaces, 8CB monolayers are preferentially oriented along the rubbing direction. The in-plane orientational anisotropy is reflected in the $\vec{\vec{\chi}}^{(2)}$ tensor for the monolayers. In this case, the nonvanishing $\vec{\vec{\chi}}^{(2)}$ elements are [5]

$$\chi^{(2)}_{zzz}=N_s\langle \sin^3\theta_m \rangle\alpha^{(2)}_{\zeta\zeta\zeta} ,$$
$$\chi^{(2)}_{zyy}=\chi^{(2)}_{yzy}=N_s\langle \sin\theta_m \cos^2\theta_m \rangle\langle \sin^2\phi_m \rangle\alpha^{(2)}_{\zeta\zeta\zeta} ,$$
$$\chi^{(2)}_{zxx}=\chi^{(2)}_{xzx}=N_s\langle \sin\theta_m \cos^2\theta_m \rangle\langle \cos^2\phi_m \rangle\alpha^{(2)}_{\zeta\zeta\zeta} ,$$
$$\chi^{(2)}_{xxx}=N_s\langle \cos^3\theta_m \rangle\langle \cos^3\phi_m \rangle\alpha^{(2)}_{\zeta\zeta\zeta} , \quad (3)$$
$$\chi^{(2)}_{xzz}=N_s\langle \cos\theta_m \sin^2\theta_m \rangle\langle \cos\phi_m \rangle\alpha^{(2)}_{\zeta\zeta\zeta} ,$$
$$\chi^{(2)}_{xyy}=N_s\langle \cos^3\theta_m \rangle\langle \sin^2\phi_m \cos\phi_m \rangle\alpha^{(2)}_{\zeta\zeta\zeta} .$$

Here again, we assumed that $\vec{\vec{\alpha}}^{(2)}$ is dominated by $\alpha^{(2)}_{\zeta\zeta\zeta}$ with $\hat{\zeta}$ along the long molecular axis pointing out from the surface. We have also taken $\hat{\mathbf{x}}$ to be along the rubbing direction and $\phi_m$ to be the azimuthal angle from $\hat{\mathbf{x}}$. We have deduced these nonvanishing $\chi^{(2)}_{ijk}$ for 8CB monolayers on the different polyimide-coated surfaces from SHG measurements with different polarization combinations as functions of the azimuthal angle between the plane of incidence and the rubbing direction. A typical set of data is shown in Fig. 3, together with the theoretical fit that determines the values of $\chi^{(2)}_{ijk}$. The fitting procedure follows that of Ref. [5]. Note that $\chi^{(2)}_{zxx}$ can be directly deduced from the SH signal with the (s in–p out) polarization combination and the plane of incidence along $\hat{\mathbf{y}}$. Also, $\frac{1}{2}(\chi^{(2)}_{zxx}+\chi^{(2)}_{zyy})$ in the rubbed case should be equal to $\chi^{(2)}_{zyy}$ in the unrubbed case and $\chi^{(2)}_{zzz}$ is the same in both cases if the tilt angle $\theta_m$ remains unchanged. They can be used as starting points of the fitting procedure. Because of the larger number of data points involved in the fitting in the rubbed case, the deduced values of $\chi^{(2)}_{ijk}$ have much smaller mean square deviations than in the unrubbed case.

We now assume the monolayer orientational distribution to be

$$P(\theta_m,\phi_m)=f(\theta_m)g(\phi_m) , \quad (4)$$

with

$$f(\theta_m)=\exp[-(\theta_m-\theta_0)^2/2\sigma^2]$$

and

$$g(\phi_m)=1+d_1\cos(\phi_m)+d_2\cos(2\phi_m)+d_3\cos(3\phi_m) .$$

Substitution of Eq. (4) into Eq. (3) with the measured values of $\chi^{(2)}_{ijk}$ allows us to deduce $\theta_m$, $\sigma$, $d_1$, $d_2$, and $d_3$. The results for 8CB monolayers on four different polyimide-coated substrates are listed in Table I. All parameters except $d_3$, which is almost negligible, exhibit an odd-even effect. The tilt angle $\theta_m$ is essentially the same as in the unrubbed case; the width of $f(\theta_m)$ is significantly larger for 8CB on polyimides with even numbers of spacer units. For the azimuthal distribution $g(\phi_m)$, $d_1$ describes the forward-backward asymmetry and $d_2$ describes the $\hat{\mathbf{x}}$-$\hat{\mathbf{y}}$ anisotropy. The latter appears to have a much stronger odd-even effect.

## IV. DISCUSSION

The odd-even effect exhibited by 8CB monolayers on polyimides must be related to the surface structures of polyimides. As shown by Yokokura *et al.* using x-ray scattering and scanning electron microscopy [8], surfaces of polyimides with odd numbers of spacer units are more corrugated, presumably because the neighboring aromatic units are oriented differently and crystallization is hindered. We believe that 8CB molecules adsorbed on such surfaces would more or less follow the local surface morphology and therefore have a higher average tilt angle. This is different from polyimides with even numbers of spacer units. Their surfaces are smoother and tend to crystallize because neighboring aromatic units favor parallel orientation. The tilt angle of adsorbed 8CB is likely to be smaller. This picture is in agreement with the result we have obtained as described in the preceding section, but at variance with the picture suggested by Yokokura *et al.* [8].

Aside from the odd-even effect, the tilt angle tends to be smaller on polyimides with larger numbers of spacer units. This may be expected by the consideration that the longer and rather flexible section could make the polyimide surface smoother. We also notice that on the rubbed polyimide surfaces, the spread $\sigma$ of the tilt angle

$\theta_m$ of 8CB is significantly larger for polyimides with even numbers of spacer units, although their surfaces are smoother. This seems to be correlated with the stronger anisotropy in the azimuthal orientational distribution as seen in Table I. It is known that rubbing could induce alignment of the surface polymer chains and is most effective if the polymer surface is crystalline [10]. Crystallinity of a polymer surface has been shown to be of crucial importance in the construction of a well-aligned homogeneous liquid crystal cell [10]. Since polyimides have a clear odd-even effect in their ability to crystallize, we can easily understand why the anisotropic $d_2$ coefficient in $g(\phi_m)$ is larger for 8CB on polyimides with even numbers of spacer units. It is possible that with more 8CB molecules oriented around $\pm\hat{\mathbf{x}}$, steric interaction between 8CB molecules forces them to spread out more in $\theta$, yielding a larger value of $\sigma$. The coefficients $d_1$ and $d_3$ in $g(\phi_m)$ of Eq. (4) describe the forward-backward asymmetry along the rubbing direction $\hat{\mathbf{x}}$. This asymmetry arises only because the polyimide surfaces were rubbed along one direction ($+\hat{\mathbf{x}}$) [5]. The odd-even effect in this case is not expected to be appreciable. If anything, polyimide surfaces with more crystallinity or ordering, i.e., polyimides with even numbers of spacer units, should have stronger asymmetry. This is indeed the case we have observed as indicated in Table I.

The question yet to be answered is why the observed odd-even effect in the bulk tilt angle $\theta_B$ is opposite to that of the adsorbed monolayer $\theta_m$. We provide here a plausible explanation. First, we realize that we need to relate the surface LC molecular orientation with the macroscopic surface order parameter. This can be achieved by knowing $P(\theta_m,\phi_m)$ in the rubbed polyimide cases. Because of alignment in both polar and azimuthal directions, the tensor order parameter is biaxial. Second, the surface order parameter must relax towards a uniaxial order parameter in the bulk. In the surface-bulk transition region, the gradient of the order parameter induces a splay distortion via the anisotropic order elasticity. The uniaxial direction of the bulk order parameter is then tilted away from the surface plane depending to some extent on the surface ordering. Finally in the bulk, the optically

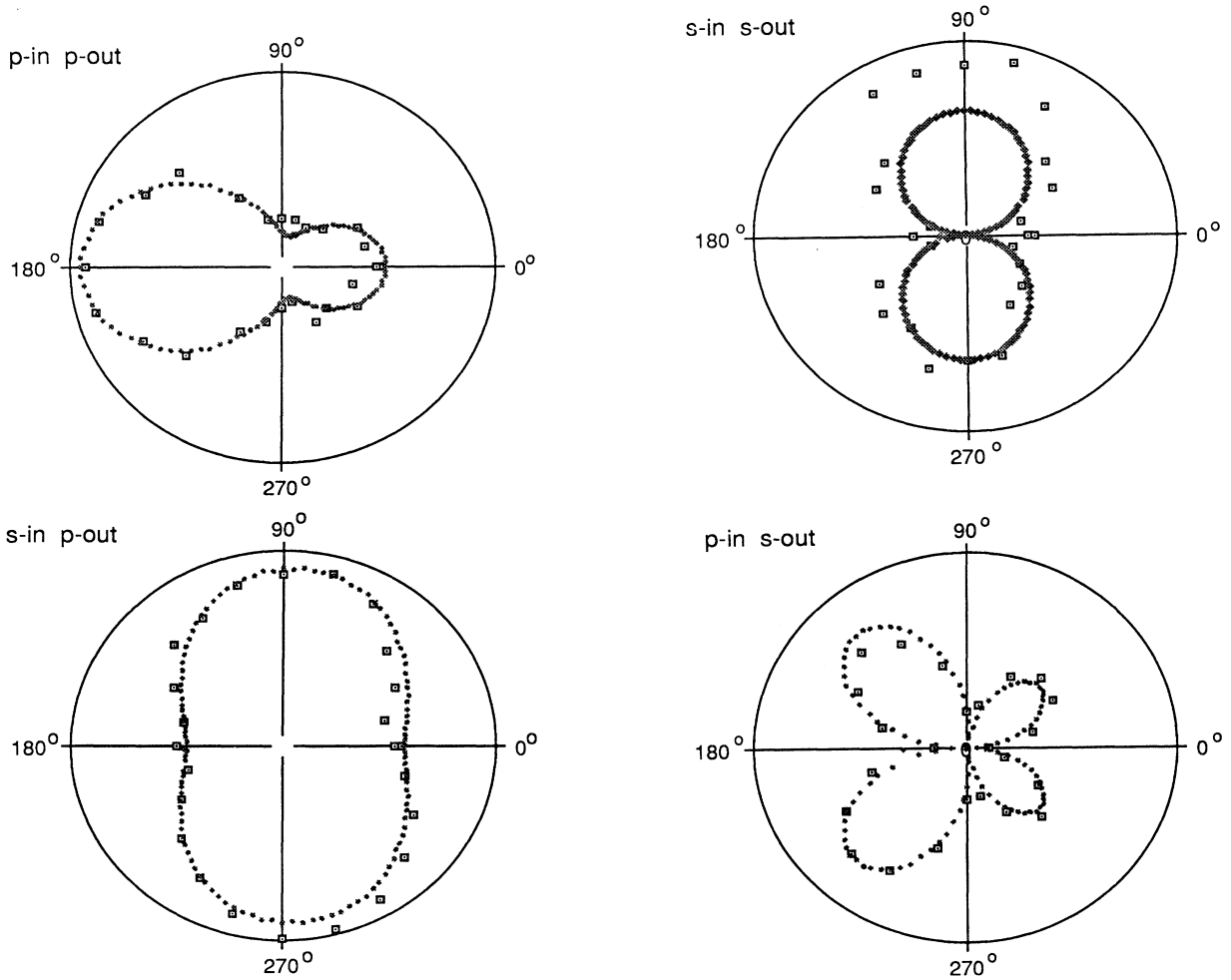


FIG. 3. Square root of the second-harmonic signal (arbitrary units) vs the angle between the rubbing direction and the plane of incidence for four different input-output polarization combinations: ($p$ in $p$ out) refers to $p$-polarized fundamental input and a $p$-polarized second-harmonic output. The sample is an 8CB monolayer on a rubbed P5-coated substrate.

TABLE I. Parameters describing molecular orientational distributions of 8CB monolayers on the four rubbed polyimide surfaces. For definitions of the orientational moments see Eq. (4).

| Type of polyimide | | P3 | P4 | P5 | P6 |
|---|---|---|---|---|---|
| Molecular tilt angle | $\theta_m$ | 18° | 14° | 16° | 12° |
| Spread in tilt angle | $\sigma(\theta)$ | 1° | 9° | 4° | 6° |
| Moments of in-plane orientational order | $d_1$ | 0.20 | 0.23 | 0.18 | 0.35 |
| | $d_2$ | 0.32 | 0.89 | 0.55 | 0.89 |
| | $d_3$ | 0.01 | 0.02 | 0.02 | 0.07 |

measured molecular tilt angle is just the tilt angle of the uniaxis of the order parameter. The above picture predicts that $\theta_B$ would be larger if the surface ordering is higher. This is the case with surfaces coated by polyimides with even numbers of spacer units. In this respect the odd-even effect of $\theta_B$ is directly related to the crystallinity of the polyimide surface, but only indirectly to the odd-even effect in $\theta_m$.

To substantiate the above picture, we carry out the following calculations. We define the order parameter in the usual way [13],

$$Q_{ij}=\langle \tfrac{1}{2}(3n_in_j-\delta_{ij})\rangle \ , \tag{5}$$

where $n_x=\cos\theta_m\cos\phi_m$, $n_y=\cos\theta_m\sin\phi_m$, $n_z=\sin\theta_m$, and the angular brackets denote an average over the molecular orientational distributions. For 8CB molecules on the rubbed polyimide surfaces, we have deduced from our experiment the approximate orientational distributions $P(\theta_m,\phi_m)$ expressed in Eq. (4) with coefficients listed in Table I. It is then possible to calculate the surface order parameter $\overleftrightarrow{Q}^S$ using Eq. (5). The resultant $\overleftrightarrow{Q}^S$ is not diagonalized in the $\hat{x}$-$\hat{y}$-$\hat{z}$ laboratory coordinates, but can be diagonalized in the $\hat{x}'$-$\hat{y}'$-$\hat{z}'$ coordinates into the form

$$\overleftrightarrow{Q}^S=\begin{bmatrix} S_s & 0 & 0 \\ 0 & \dfrac{-(S_s-P_s)}{2} & 0 \\ 0 & 0 & \dfrac{-(S_s+P_s)}{2} \end{bmatrix} \tag{6}$$

typical for a biaxial layer, where $S_s$ and $P_s$ are the two scalar order parameters describing the biaxial ordering. In the diagonalization process, the angle $\theta_s$ between $\hat{x}'$ and $\hat{x}$ (or $\hat{z}'$ and $\hat{z}$) can also be deduced. The values of $S_s$, $P_s$, and $\theta_s$ thus obtained for the four different polyimide surfaces are given in Table II. Note that the odd-even effect in the scalar surface order parameters $S_s$ and $P_s$ is much more apparent than in the values describing the molecular orientation in Table I. This is presumably because the surface order parameters more truly represent the surface-induced effect. On the other hand, the clear odd-even effect present in the tilt angle $\theta_m$ does not translate into a corresponding odd-even effect in $\theta_s$. This is because averaging over the azimuthal angle partially smears the effect. Note that for a monolayer with in-plane isotropy, one expects $\theta_s=0$ irrespective of the value of $\theta_m$.

TABLE II. Surface order parameters after diagonalization as derived from the orientational distributions of the LC monolayers given in Table I and Eq. (5). For definitions of the parameters see Eq. (6).

| Type of polyimide | P3 | P4 | P5 | P6 |
|---|---|---|---|---|
| $S_s$ | 0.29 | 0.49 | 0.38 | 0.53 |
| $P_s$ | 0.43 | 0.26 | 0.38 | 0.32 |
| $\theta_s$ | 3.9 | 2.8 | 2.7 | 3.2 |

Surface ordering described by $S_s$, $P_s$, and $\theta_s$ is expected to relax towards bulk ordering described by $S_B$, $P_B=0$, and $\theta_B$ over a surface-bulk transition region. How these parameters vary across this transition layer can be determined by minimization of the Landau–de Gennes free energy [13] given by

$$F=\int dV(f_u+f_g) \ , \tag{7}$$

with

$$f_u=\frac{a^*(T-T^*)}{2}Q_{ij}Q_{ij}-\frac{B}{3}Q_{ij}Q_{jk}Q_{ki} +\frac{C_1}{4}Q_{ij}Q_{ij}Q_{kl}Q_{kl}+\frac{C_2}{4}Q_{ij}Q_{jk}Q_{kl}Q_{li} \ ,$$

$$f_g=\frac{1}{2}L_1\frac{\partial}{\partial k}Q_{ij}\frac{\partial}{\partial k}Q_{ij}+\frac{1}{2}L_2\frac{\partial}{\partial k}Q_{ik}\frac{\partial}{\partial k}Q_{ik} \ ,$$

where $a^*$, $T^*$, $B$, $C_1$, $C_2$, $L_1$, and $L_2$ are material constants [14,15] and $T$ is the temperature. The $f_g$ part accounts for order elasticity with the anisotropic part described by the $L_2$ term. Several authors have included an interface term $f_s$, which after minimization determines the surface order parameter $\overleftrightarrow{Q}^S$ [16]. Here, however, we treat $\overleftrightarrow{Q}^S$ as a known quantity obtained directly from experiment.

In order to focus on the surface-bulk transition, we write

$$\begin{aligned} f_u&=\tfrac{1}{2}A(Q-Q^B)_{ij}(Q-Q^B)_{ij}+f_b \\ &=\tfrac{1}{2}A_S(S-S_B)^2+\tfrac{1}{2}A_PP^2+f_b \end{aligned} \tag{8}$$

neglecting higher-order terms in the series expansion, where

$$A_S=\tfrac{3}{2}a^*(T-T^*)-\tfrac{3}{2}BS_B+\tfrac{27}{4}(C_1+\tfrac{1}{2}C_2)S_B^2 \ ,$$

$$A_P=\tfrac{1}{2}a^*(T-T^*)+\tfrac{1}{2}BS_B+\tfrac{3}{4}(C_1+\tfrac{1}{2}C_2)S_B^2 \ ,$$

and $f_b$ is the free energy density of the uniform bulk with $F_b=\int f_b dV$. The free energy to be minimized is now

$$F-F_B=\int dV\left[\frac{A_S}{2}(S-S_B)^2+\frac{A_P}{2}P^2 +\frac{L_1}{2}\frac{\partial}{\partial k}Q_{ij}\frac{\partial}{\partial k}Q_{ij} +\frac{L_2}{2}\frac{\partial}{\partial k}Q_{ik}\frac{\partial}{\partial k}Q_{ik}\right] . \tag{9}$$

Order electricity and flexo electricity [17–21] are included in this free energy insofar as the polarization is originated from a divergence of the quadrupole density [18,19]. In this quadrupolar picture the polarization is written as $\mathbf{P}_{el}=-\nabla\cdot(\overleftrightarrow{Q}_{el})$, where $\mathbf{P}_{el}$ is the polarization and $\overleftrightarrow{Q}_{el}$ is the quadrupole density, which is proportional to the order parameter $\overleftrightarrow{Q}$. The corresponding term in the free-energy density is $f_{el}=(1/2\varepsilon)P_{el}^2=(1/2\varepsilon)(\partial Q_{ik}/\partial k)(\partial Q_{ik}/\partial k)$, where $\varepsilon$ is the dielectric constant. Comparison with Eq. (9) shows that $f_{el}$ has the same structure as the $L_2$ term dealing with the anisotropic order elasticity. Thus the $L_2$ term in Eq. (9) also includes the electrical contribution to the anisotropic order elasticity.

To illustrate the picture of the surface-bulk transition, we outline in the following the derivation with the biaxiality $P$ neglected for clarity. We find $Q_{ij}$ in the laboratory frame as

$$\overleftrightarrow{Q}=\begin{bmatrix} \frac{2\cos^2\theta-\sin^2\theta}{2}S & 0 & \frac{-3\cos\theta\sin\theta}{2}S \\ 0 & \frac{-S}{2} & 0 \\ \frac{-3\cos\theta\sin\theta}{2}S & 0 & \frac{2\sin^2\theta-\cos^2\theta}{2}S \end{bmatrix} . \quad (10)$$

Inserting Eq. (10) into Eq. (9) and keeping $\theta$ to second order yields

$$F-F_B=\frac{1}{2}A_S(S-S_B)^2+\frac{3}{4}\left[L_1+\frac{L_2}{6}\right]S'^2+\frac{3}{8}L_2S'^2\theta^2 +\frac{9}{4}\left[L_1+\frac{L_2}{2}\right]S^2\theta'^2+\frac{3}{4}L_2SS'\theta\theta' , \quad (11)$$

where primes denote derivatives with respect to $z$. The last term in Eq. (11) couples gradients with $\theta$ and $S$ via the anisotropic order elasticity. Since $S$ and $\theta$ are positive, minimization of the free energy involving this term will always favor an opposite sign of $S'$ and $\theta'$. This means that the tilt would go up, if $S$ goes down along $z$ and vice versa. This will be seen more explicitly in the derivation.

The Euler-Lagrange equations derived from $F-F_B$ in Eq. (11) are

$$\frac{3}{2}\left[L_1+\frac{L_2}{6}+\frac{L_2}{2}\theta^2\right]S''+\frac{3L_2}{2}\theta\theta'S' -\left[A_S+\left[\frac{9L_1}{2}+\frac{3L_2}{2}\right]\theta'^2-\frac{3L_2}{4}\theta\theta''\right]S +A_SS_B=0 \quad (12)$$

and

$$\frac{9}{2}\left[L_1+\frac{L_2}{2}\right]S^2\theta''+9\left[L_1+\frac{L_2}{2}\right]SS'\theta'+\frac{3L_2}{4}SS''\theta=0 . \quad (13)$$

In the approximate calculation, we decouple Eq. (12) from Eq. (13) by noting that $\theta\ll 1$ and all derivatives of $\theta$ occur on a length scale comparable to the length scale for changes in $S$. We then have, instead of Eq. (12),

$$\frac{3}{2}\left[L_1+\frac{L_2}{6}\right]S''-A_S(S-S_B)=0 , \quad (14)$$

which has a solution

$$S(z)=S_B+\Delta S_S\exp(-z/\xi) , \quad (15)$$

where $\Delta S_S=S_S-S_B$ and $\xi=\sqrt{\frac{3}{2}(L_1+L_2/6)/A_S}$ is the correlation length, $S_B\sim 0.6$ [14], and $S_S$ is given in Table II. Equation (15) is then inserted in Eq. (13), with the approximation $\Delta S(z)=S(z)-S_B\ll S_B$, to yield

$$\theta''+a(z)\theta'+b(z)\theta=0 , \quad (16)$$

with

$$a(z)=\frac{-2\Delta S(z)}{S_B\xi},\quad b(z)=\frac{L_2}{6K_1}\frac{\Delta S(z)}{S_B\xi^2} , \quad (17)$$

where $\Delta S(z)=S(z)-S_B$ and $K_1=L_1+L_2/2$. Equation (16) can be solved with the boundary conditions $\theta=\theta_S$ at $z=0$ and $\theta'=0$ as $z\to\infty$. The detailed calculation leads to

$$\theta_B=\theta_S\beta\exp\left[\frac{\Delta S_S}{S_B}\right] , \quad (18)$$

with

$$\beta=\frac{1}{\cosh(\alpha)},\quad \alpha=-\frac{b_0^2}{a_0^2C}+\frac{C}{4}-\frac{b_0}{a_0}\ln\left[\frac{a_0C}{-2b_0}\right] ,$$
$$C=a_0-\frac{2b_0}{a_0}+\sqrt{a_0^2-4b_0},\quad a_0=\frac{-2\Delta S_S}{S_B} , \quad (19)$$
$$b_0=\frac{L_2}{6K_1}\frac{\Delta S_S}{S_B} .$$

It turns out that $\beta$ has a value close to 1, which is only weakly dependent on the surface ordering. Equation (18) very clearly illustrates that a change in the surface order parameter $S_S$ is connected to a change in the tilt angle $\theta_B$.

We can also include the biaxial order parameter $P$ in the calculation by assuming that $S$ and $P$ have the same correlation length, i.e., $A_S\sim A_P$. In this case the Euler-Lagrange equation for $\theta$ becomes

$$\frac{9}{2}\left[L_1+\frac{L_2}{2}\right]\left[S+\frac{P}{3}\right]^2\theta''+9\left[L_1+\frac{L_2}{2}\right]\left[S+\frac{P}{3}\right] \times\left[S'+\frac{P'}{3}\right]\theta'+\frac{3}{4}L_2\left[S+\frac{P}{3}\right](S''-P'')\theta=0 . \quad (20)$$

With the same approximation used to obtain Eq. (16), we find

$$\theta_B=\theta_S\beta'\exp\left[\frac{\Delta S_S+P_S/3}{S_B}\right] , \quad (21)$$

where $\beta'$ is given by Eq. (19) with $a_0$ and $b_0$ replaced by

$$a_0' = \frac{-2(\Delta S_S + P_S/3)}{S_B}, \quad b_0' = \frac{L_2}{6K_1}\frac{\Delta S_S - P_S}{S_B} . \quad (22)$$

Both Eqs. (18) and (21) predict that $\theta_B$ would increase with $\Delta S_S$ and $\theta_S$. In the present case, polyimides with even numbers of spacer units yield larger $\Delta S_S$ but do not vary $\theta_S$ appreciably. This explains the odd-even effect on $\theta_B$. Physically, it is the anisotropic order elasticity that provides the positive correlation between $\Delta S_S$ and $\theta_B$. There is also a positive correlation between the in-plane forward-backward asymmetry $d_1$ in the orientational distribution and $\theta_S$, assuming $\theta_m$ fixed. With $\theta_m$ varied for molecules on different polyimides as in our case, however, the correlation may become less obvious.

Using the values of the parameters in Table II and $L_1 = 2.0 \times 10^{-12}$ J/m, $L_2 = 4.7 \times 10^{-12}$ J/m [14], we find $\theta_B$ to be 1.9°, 2.2°, 1.6°, and 2.7° for P3, P4, P5, and P6, respectively. Figure 4 shows the experimentally found values of $\theta_B$ in comparison with the above calculated values as well as the values of $\theta_S$ and $\theta_m$. The calculation is not in good quantitative agreement with experiment. This is certainly expected knowing that our calculation is crude. We emphasize that the calculation is only meant to illustrate that the proposed mechanism can be of importance and qualitatively explain the odd-even effect observed in the bulk tilt angle.

## V. CONCLUSION

We have measured the tilt angles of the liquid-crystal molecules 8CB at the surface and in the bulk of LC cells with surfaces coated by a homologous series of polyimides. We found that the tilt angle, the in-plane anisotropy of adsorbed LC monolayers, and the tilt angle of bulk alignment all exhibit an odd-even effect associated with the odd or even number of spacer units in the polyimides. All the observations can be qualitatively understood in terms of the fact that polyimide surfaces with even numbers of spacer units are smoother, more crystalline, more ordered upon rubbing, and capable of inducing higher surface ordering in the 8CB surface layer. Indeed our experiment showed that on polyimide with an even number of spacer units, the 8CB monolayer lies flatter on the surface, and if the surface is rubbed, has a better in-plane alignment and a higher surface order parameter. The better in-plane alignment tends to lead to a higher tilt of the surface order parameter. The higher surface ordering induces a larger splay in the molecular orientation across the surface-bulk transition region because of the existence of anisotropic order elasticity. This provides a qualitative explanation of why the tilt angle of the bulk orientation appears to be larger in 8CB cells with surfaces coated by polyimides with an even number of spacer units.

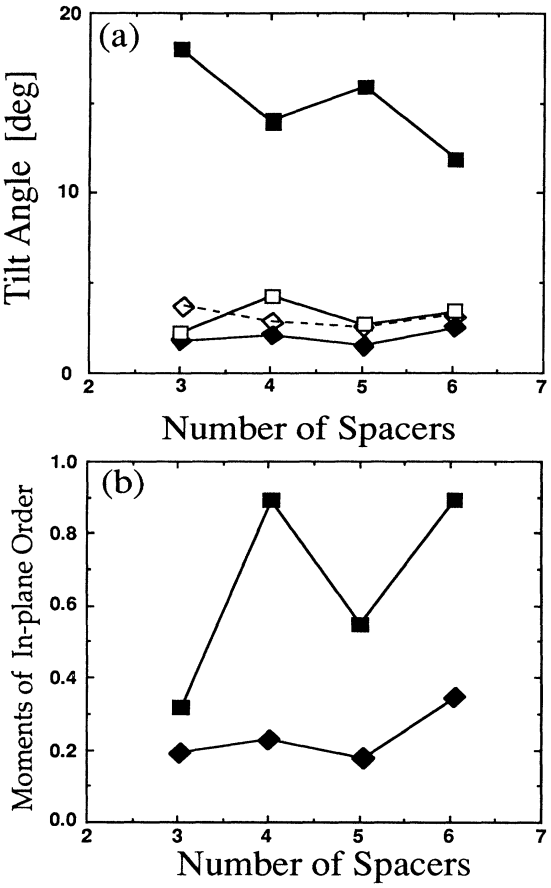


FIG. 4. Summary of results and comparison with theory. (a) Surface molecular tilt angles $\theta_m$ (filled squares), bulk tilt angles $\theta_B$ as measured (open squares), tilt angles $\theta_S$ of the surface order parameter as in Table II (open diamonds, dashed line), and bulk tilt angles as calculated from Eq. (21) and Table II (filled diamonds). (b) First (filled diamonds) and second (filled squares) moments of in-plane orientational order at the surface $d_1$ and $d_2$ as in Table I.

## ACKNOWLEDGMENTS

This work was supported by NSF Grant No. DMR-9025106. D.J. and H.W. gratefully acknowledge financial support from the Alexander-von-Humboldt Foundation and the AIO network, respectively.

*Permanent address: Max-Planck-Institut fuer Polymerforschung, Ackermannweg 10, D-55021 Mainz, Federal Republic of Germany.

†Present address: Department of Physics and Astronomy, Northwestern University, 2145 Sheridan Rd., Evanston, IL 60208-3112.

‡Permanent address: Institute of Physics, University of Aalborg, Pontoppidanstraede 103, DK 9220 Aalborg Ost, Denmark.

§Permanent address: Faculty of Science, University of

Nijmegen, Toernooiveld, 6525ED Nijmegen, The Netherlands.

**Permanent address: Autodisplay a.s., P. O. Box 240, Thorøya, N3201 Sandefjord, Norway.

[1] For a recent review see, e.g., B. Jerômé, Rep. Prog. Phys. **54**, 391 (1991).

[2] H. Yokoyama, Mol. Cryst. Liq. Cryst. **165**, 265 (1988).

[3] J. Cognard, *Alignment of Liquid Crystals and their Mixtures* (Gordon and Breach, London, 1982).

[4] B. S. Scheuble, Kontakte **1**, 34 (1989).

[5] M. B. Feller, W. Chen, and Y. R. Shen, Phys. Rev. A **43**, 6778 (1991).

[6] W. Chen, M. B. Feller, and Y. R. Shen, Phys. Rev. Lett. **63**, 2665 (1989).

[7] J. M. Geary, J. W. Goodby, A. R. Kmetz, and J. S. Patel, J. Appl. Phys. **62**, 4100 (1987).

[8] H. Yokokura, M. Oh-E, K. Kondo, and S. Oh-Hara, Mol. Cryst. Liq. Cryst. **225**, 253 (1993).

[9] See, e.g., Y. R. Shen, Annu. Rev. Phys. Chem. **40**, 327 (1989); Nature (London) **337**, 4480 (1990).

[10] B. O. Myrvold, Liq. Cryst. **10**, 771 (1991).

[11] Y. R. Shen, Liq. Cryst. **5**, 635 (1989).

[12] B. Jerômé and P. Pieranski, J. Phys. (Paris) **49**, 1601 (1988).

[13] See, e.g., P. Sheng and E. B. Priestley, in *Introduction to Liquid Crystals,* edited by E. B. Priestley, P. J. Wojtowicz, and P. Sheng (Plenum, New York, 1974), Chap. 10.

[14] N. V. Madhusudana and R. Pratibha, Mol. Cryst. Liq. Cryst. **89**, 249 (1982).

[15] H. J. Coles, Mol. Cryst. Liq. Cryst. **49**, 67 (1978). Note that this reference uses different definitions: $a^{*}_{\text{Coles}} = \frac{3}{2}a^{*}$, $b_{\text{Coles}} = \frac{3}{4}B$, $c_{\text{Coles}} = \frac{9}{4}(C_1 + \frac{1}{2}C_2)$.

[16] See, e.g., T. J. Sluckin and A. Poniewierski, in *Fluid Interfacial Phenomena,* edited by C. A. Croxton (Wiley, New York, 1985).

[17] G. Barbero, I. Dozov, J. F. Palierne, and G. Durand, Phys. Rev. Lett. **56**, 2056 (1986). In general, order and flexo electricity connected to a surface-induced dipolar order can also contribute to the behavior we have observed. Unfortunately, the four material parameters describing order and flexo electricity are not known to sufficient precision for 8CB. However, it is expected that the different constants are similar to each other in value. If this is the case, the picture is not changed.

[18] G. Durand, Physica A **163**, 94 (1990).

[19] J. Prost and J. P. Marcerou, J. Phys. (Paris) **38**, 315 (1977).

[20] I. Janossy, Europhys. Lett. **5**, 431 (1988).

[21] R. B. Meyer, Phys. Rev. Lett. **22**, 918 (1969).